© 2016. Published by The Company of Biologists Ltd | Development (2016) 143, 4676-4686 doi:10.1242/dev.136127

RESEARCH ARTICLE

Integration of actomyosin contractility with cell-cell adhesion during dorsal closure

Julia Duque and Nicole Gorfinkiel*

ABSTRACT

In this work, we combine genetic perturbation, time-lapse imaging and quantitative image analysis to investigate how pulsatile actomyosin contractility drives cell oscillations, apical cell contraction and tissue closure during morphogenesis of the amnioserosa, the main force-generating tissue during the dorsal closure in *Drosophila*. We show that Myosin activity determines the oscillatory and contractile behaviour of amnioserosa cells. Reducing Myosin activity prevents cell shape oscillations and reduces cell contractility. By contrast, increasing Myosin activity increases the amplitude of cell shape oscillations and the time cells spend in the contracted phase relative to the expanded phase during an oscillatory cycle, promoting cell contractility and tissue closure. Furthermore, we show that in AS cells, Rok controls Myosin foci formation and Mbs regulates not only Myosin phosphorylation but also adhesion dynamics through control of Moesin phosphorylation, showing that Mbs coordinates actomyosin contractility with cell-cell adhesion during amnioserosa morphogenesis.

KEY WORDS: Actomyosin, Adhesion, Apical contraction, Oscillations

INTRODUCTION

Morphogenesis refers to the coordinated set of tissue movements that generate biological shape. The regulated activity of the cytoskeleton induces cell shape changes by coupling to the inter-cellular adhesion systems that maintain tissue coherence. It remains unclear how the balance between plasticity and stability – allowing the remodelling of tissues while maintaining their integrity – is regulated during embryonic development. Recent evidence from different cell and model systems shows that adhesion and contractility driven by the actomyosin cytoskeleton are integrated at E-cadherin junctions by a combination of biochemical pathways and biomechanical feedback (Lecuit and Yap, 2015).

In various tissues undergoing morphogenesis, the actomyosin cytoskeleton forms an apical network showing periodic contractions driving cell shape oscillations (Gorfinkiel and Blanchard, 2011). In *Drosophila*, this oscillatory activity has been observed in a diverse array of tissue movements such as invagination, sealing, convergent extension and remodelling of organ shape. Work done in recent years has started to explore the origin of actomyosin oscillations and how they are stabilized and linked to the cell membrane to give rise to cell shape changes (Gorfinkiel, 2016). The regulation of Myosin activity through its phosphorylation is an important way to modulate medial actomyosin oscillatory activity. Myosin phosphorylation is regulated by Myosin kinases, including Rok, and Myosin phosphatases, suggesting that the balance between these two activities determines the levels of activated Myosin (Vicente-Manzanares et al., 2009). Interestingly, both Rok and the Myosin binding subunit (Mbs) of *Drosophila* Myosin light chain phosphatase, colocalize with Myosin in dynamic medioapical foci in *Drosophila* epidermal cells and it has been suggested that actomyosin oscillations are an emergent property of a biomechanical network involving the regulators of Myosin phosphorylation and the movement – advection – of the actomyosin network (Munjal et al., 2015). Moreover, studies with phosphomimetic and a non-phosphorylatable forms of Myosin regulatory light chain [Spaghetti squash (Sqh), in *Drosophila*] have shown that altered Myosin phosphorylation dynamics perturbs actomyosin contractions and cell shape changes (Kasza et al., 2014; Munjal et al., 2015; Vasquez et al., 2014).

Here, we tackle these questions during the morphogenesis of the amnioserosa, the main force-generating tissue during dorsal closure (Hutson et al., 2003; Kiehart et al., 2000). Amnioserosa (AS) cells undergo pulsatile apical contraction driven by the periodic formation of actomyosin foci at the apical surface of cells (Blanchard et al., 2010; David et al., 2010; Sokolow et al., 2012; Solon et al., 2009). RhoGEF2, an upstream regulator of Rho and possibly of Rok, is required for Myosin apical localization and for AS cell oscillations (Azevedo et al., 2011), suggesting that the mechanisms driving pulsatile actomyosin contractility are conserved. The frequency of appearance of Myosin foci increases as DC progresses, correlating with an increase in the rate of contraction of AS cells (Blanchard et al., 2010; Machado et al., 2015; Sokolow et al., 2012). It is not known what drives these changes but it has been proposed that a biochemical circuit involving Par proteins is involved (David et al., 2013).

Making use of Myosin mutant forms that substitute the phosphorylation site by unphosphorylatable and phosphomimetic residues (Jordan and Karess, 1997; Vasquez et al., 2014), we analyse how Myosin activity affects cell oscillations, cell contractility and tissue closure in the AS. Reducing Myosin activity prevents cell shape oscillations and reduces cell contractility. Conversely, a phosphomimetic form of Myosin increases Myosin persistence at the medioapical region of AS cells, which results in cells that spend more time in the contracted phase relative to the expansion phase during an oscillatory cycle, promoting cell and tissue contraction. Moreover, we show that Rok and Mbs regulate Myosin foci dynamics, and find that Mbs also regulates adhesion dynamics, thus acting as a coordinator of actomyosin contractility and adhesion during morphogenesis.

Centro de Biología Molecular 'Severo Ochoa', CSIC-UAM, Cantoblanco, Madrid 28049, Spain.

*Author for correspondence (ngorfinkiel@cbm.csic.es)

N.G., 0000-0002-6847-6721

Received 3 February 2016; Accepted 27 October 2016

Development (2016) 143, 4676-4686 doi:10.1242/dev.136127

RESULTS

Role of Myosin activity in Myosin foci dynamics

We analysed how Myosin activity affects Myosin foci making use of phosphomimetic and non-phosphorylatable forms of Sqh. Using antibodies against the mono-phosphorylated (Ser21) form of Sqh and the di-phosphorylated form, it has been shown that in the AS only the mono-phosphorylated form is present (Zhang and Ward, 2011) (Fig. S1A,B). Thus, to analyse the contribution of Myosin phosphorylation to Myosin foci dynamics, we used GFP-tagged forms of Sqh phosphomutants affecting serine 21 only, under the control of the *sqh* promoter (Vasquez et al., 2014). Although biochemical studies have raised some caveats for the use of these mutant variants (Heissler and Sellers, 2015), *in vivo* studies have shown that substitution of serine 21 by alanine (SqhA21) or by glutamate (SqhE21) decrease or increase, respectively, Myosin activity (Heissler and Sellers, 2015; Jordan and Karess, 1997; Kasza et al., 2014; Vasquez et al., 2014). To reduce endogenous Sqh levels, we combined Sqh phosphomutants with a hypomorphic sqh^1 mutant allele.

Both SqhA21::GFP and SqhE21::GFP (hereafter SqhA21 and SqhE21) localize in transient foci in AS cells (Fig. 1A-C; Movie 1). SqhE21 also shows a strong localization at the level of the cell membranes (Fig. 1C,C′) and during late stages of DC it forms a denser apical meshwork (Fig. 1C′). These observations suggest that mimicking Sqh phosphorylation promotes stabilization of the medioapical and junctional Myosin networks.

We measured the cycle length of Myosin foci (Fig. 1D) over a 30 min time window, in early DC stage embryos expressing SqhA21, Sqh or SqhE21 and found it was longest in SqhA21 embryos and shortest in SqhE21 embryos (Fig. 1E). This could be due to changes in the duration of foci, the time interval between consecutive foci, or both. In SqhA21 embryos, the time interval between foci is higher, but the duration of foci is statistically indistinguishable from the wild type. In contrast, the duration and the time interval of SqhE21 foci are lower (Fig. 1F,G). These results suggest that increasing Myosin activity promotes foci formation. The duration of foci is much less affected; however, we also observed that in SqhE21 embryos there is a significant increase of overlapping foci (in which the time interval is negative) and of foci that assemble immediately after the previous one has disassembled (time interval is 0). To better take into account these features, we measured the time Myosin is present in the medioapical region relative to the time there is no Myosin, which we term ‘Myosin persistence’. Interestingly, SqhE21 is more persistent and SqhA21 is less persistent than wild-type Myosin (Fig. 1H).

Altogether, these results show a correlation between Myosin activity, the cycle length of Myosin foci and Myosin persistence, with increasing Myosin persistence as Myosin activity increases. Next, we sought to investigate how this altered Myosin dynamics affects cell oscillations and cell contractility.

Role of Myosin activity in apical cell oscillations

We generated long time-lapse movies of DC embryos carrying non-tagged versions of Sqh phosphomutants (Jordan and Karess, 1997) and the knock-in DE-Cadherin::GFP allele (Fig. 2A-C″; Movies 2,3) (DE-cadherin is known as Shotgun in *Drosophila*) and quantitatively analysed cell oscillations and cell shape changes. The cycle length and amplitude of apical cell area oscillations show a temporal pattern over DC (Blanchard et al., 2010; Sokolow et al., 2012). During early DC, AS apical cell area fluctuates with long cycle lengths and high amplitudes. The onset of whole tissue contraction coincides with a decrease in both the cycle length and the amplitude of cell oscillations, and at around 50 min after the onset of AS tissue contraction, as the zippering engages, cells enter a fast mode of oscillations with low amplitude and short cycle length.

We find that the temporal pattern of the amplitude and cycle length of apical cell area oscillations is disrupted in embryos

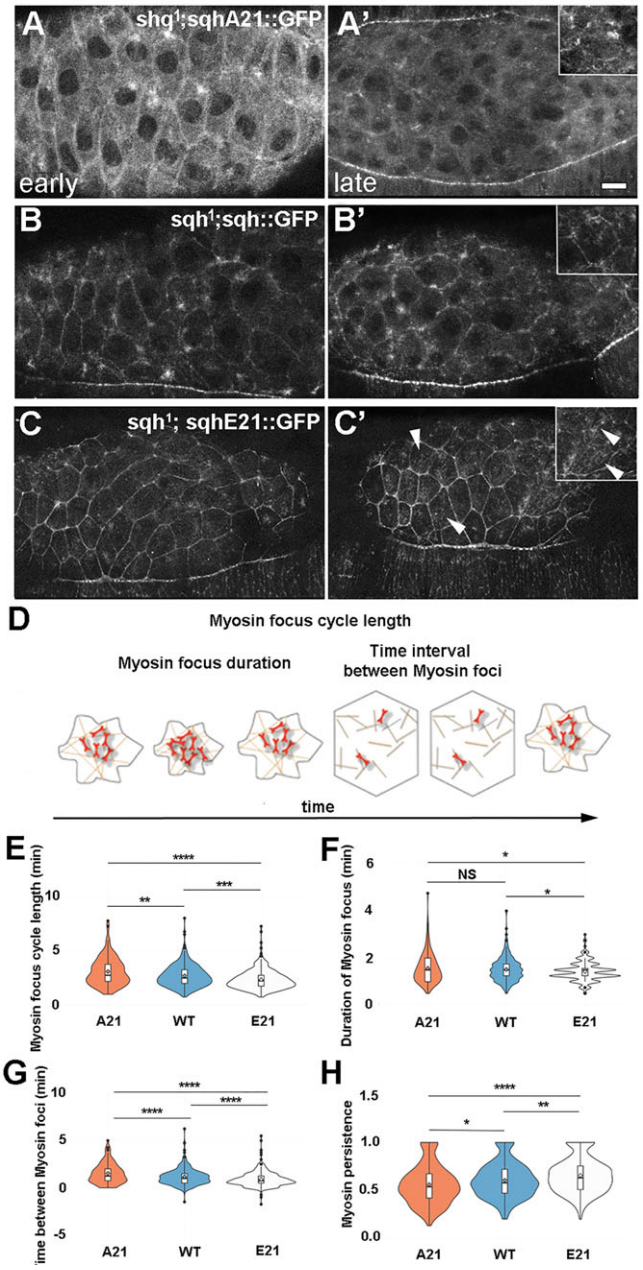

Fig. 1. Dynamics of Myosin phosphomutant foci in amnioserosa cells. (A-C′) Still images from a time-lapse movie of example sqh^1 embryos during early (A,B,C) and late (A′,B′,C′) DC carrying SqhA21::GFP (A,A′), Sqh::GFP (B,B′) and SqhE21::GFP (C,C′). Insets in A′-C′ show a magnification of an individual amnioserosa cell. Arrowheads in C′ indicate filaments formed by SqhE21::GFP. (D) Cartoon depicting the cycle length, duration, time interval and persistence of a schematic Myosin focus. (E-H) Violin plots displaying the probability density of the data at different values for the cycle length (E), duration (F), time interval (G) and persistence (H) of Myosin foci. Mean (diamond) and median (line) are indicated (see also Table S1). For quantification of Myosin foci, 17 cells from 5 SqhA21::GFP embryos, 33 cells from 7 Sqh::GFP embryos and 38 cells from 7 SqhE21::GFP embryos were selected. We performed a Mann–Whitney test to assess whether the means were significantly different. *P<0.05; **P<0.01; ****P<0.0001. Scale bar: 10 µm.

Development (2016) 143, 4676-4686 doi:10.1242/dev.136127

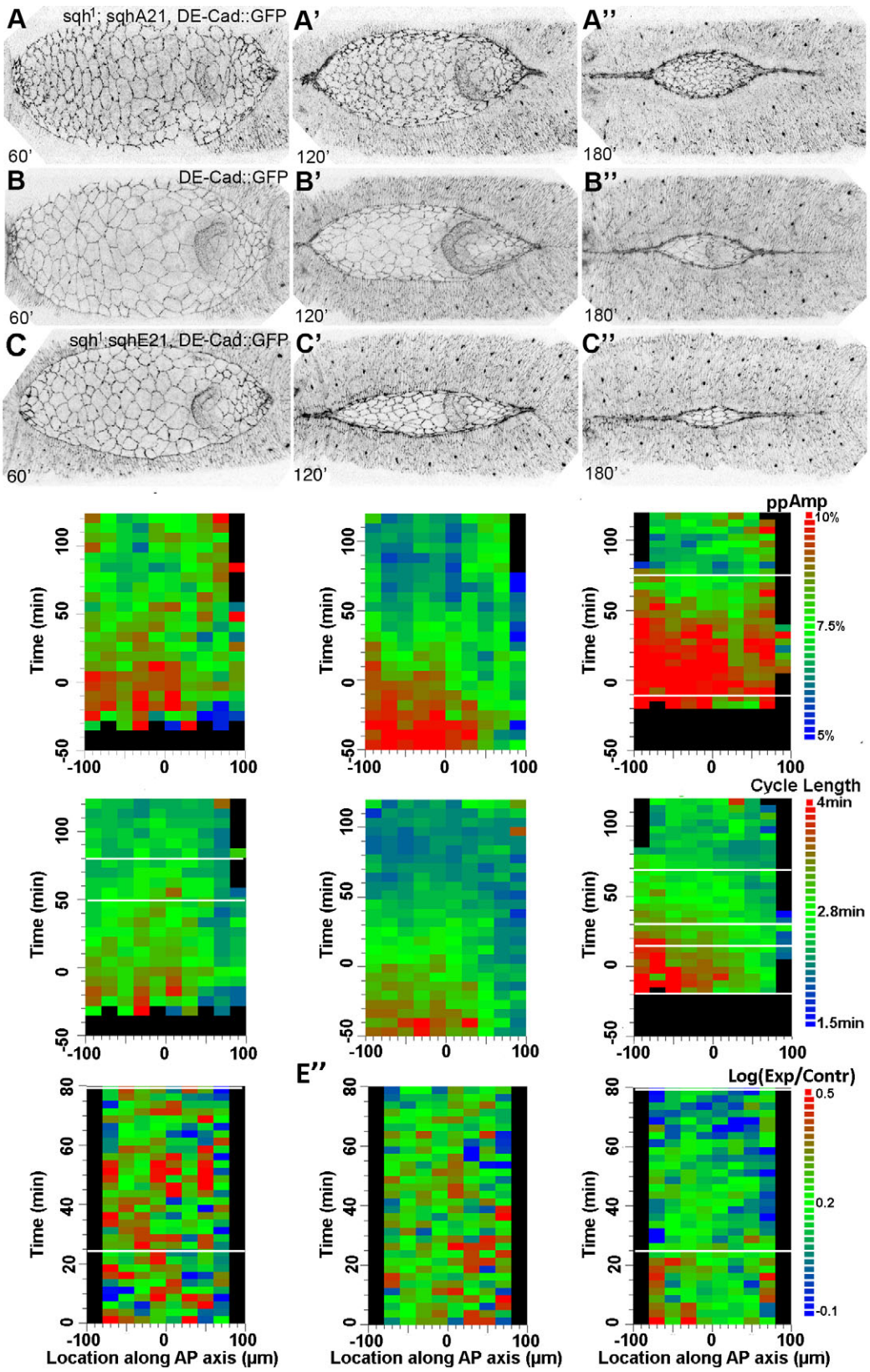

Fig. 2. Cell shape oscillations in amnioserosa cells of Sqh phosphomutants. (A-C″) Still images from a time-lapse movie of example *sqh*^{1}; DE-Cadherin::GFP embryos at 60, 120 and 180 min of DC, with SqhA21 (A-A″), wild type (B-B″) and SqhE21 (C-C″). (D-F″) Analysis of cell shape fluctuations in data pooled from 5 SqhA21 (D-D″), 7 wild-type (E-E″) and 4 SqhE21 embryos (F-F″). Average cells per embryo: 37 cells in SqhA21, 35 cells in wild-type and 53 cells in SqhE21 embryos, sampled every 30 s. (D-F) Average proportional amplitude of AS cells as a function of their location along the antero-posterior (AP) axis over time. Anterior is to the left in all similar panels. White lines show regions of significant differences between genotypes. (D′-F′) Average cycle length as a function of their AP location over time. (D″-F″) Log ratio of expansion half-cycle to contraction half-cycle durations of AS cell oscillations as a function of their AP location over time.

Development (2016) 143, 4676-4686 doi:10.1242/dev.136127

carrying Sqh phosphomutants (Fig. 2D-F′; Fig. S1D-G). We observe that the amplitude of cell shape oscillations in SqhE21 embryos is significantly greater than in wild-type cells (Fig. 2E,F; Fig. S1G), suggesting that a more active Myosin motor is able to generate a greater deformation of the apical surface area. In contrast, in SqhA21 cells, amplitudes are indistinguishable from the wild type (Fig. 2D,E; Fig. S1F), suggesting that in these embryos, there is enough Myosin activity to drive cell deformation, which could result from phosphorylation of threonine at position 20 becoming critical (Jordan and Karess, 1997).

Regarding the cycle length of cell shape oscillations, neither SqhA21 nor SqhE21 cells exhibit the fast oscillatory behaviour typical of the fast phase of DC (Fig. 2D′-F′; Fig. S1D,E). This result suggests that for cells to oscillate fast, Myosin must be able to cycle between the phosphorylated and de-phosphorylated states, and this is prevented when proteins are locked in one phosphorylation state. The cycle length of AS cell area oscillations was also different between wild-type and SqhE21 cells early during DC, with SqhE21 cells showing significantly longer periods than wild-type cells (Fig. S1E). This result is in contrast with the shortest duration of Myosin focus cycle length in SqhE21 cells, but correlated with the increased Myosin persistence. If the increase in Myosin persistence were producing an increase in the period of cell shape oscillations, we would expect that the contraction phase of the oscillatory cycle is longer than the expansion phase. Decomposing the oscillatory cycle in its contraction and expansion half-cycles, we observe that in SqhE21 cells the period of the contraction half-cycle increases more consistently than the expansion half-cycle (Fig. S2A′,B′). In contrast, in SqhA21 phosphomutants, there is a slight increase in the expansion half-cycle compared with the contraction half-cycle (Fig. S2A,B) during late stages of DC. These results show that the shape of the oscillation cycle in the phosphomutants may be affected. We have previously shown that cell oscillation cycles are asymmetric, with expansion half-cycles longer than contraction half-cycles, but this asymmetry decreases as DC progresses (Blanchard et al., 2010). We calculated the ratio of the expansion half-cycle to the contraction half-cycle times (Fig. 2D″-F″; Fig. S1H-J) and found it tends to be greater in SqhA21 than in SqhE21 cells, with wild-type cells showing an intermediate behaviour, further confirming the asymmetry of the cell oscillatory cycle in the phosphomutants. These results suggest that mimicking a permanent state of Myosin phosphorylation increases Myosin persistence, giving rise to cells that spend more time in the contracted than in the expanded state.

Linking molecular dynamics, cell contractile behaviour and tissue closure

Next, we analysed how AS cell shape and contractility were affected. As a way to assess the contractile status of AS cells, we measured their apical cell area and perimeter. During the first half of DC, AS cells from SqhA21 embryos tend on average to have greater apical cell area than wild-type cells, while SqhE21 cells are smaller (Fig. 3A-C; Fig. S3A,B). We also observe that as DC progresses, the former develop a very corrugated appearance (Fig. 2A′). Measurement of the apical cell perimeter shows that it is longer in SqhA21 embryos (Fig. 3A′-B′; Fig. S3C). This is not only a consequence of the differences in apical cell size, since the ratio of the cell perimeter to cell area also follows the same trend (Fig. 3A″,B″; Fig. S3E), indicating that for the same area, SqhA21 cells have greater perimeter than wild-type cells. Conversely, AS cells from SqhE21 embryos have smaller perimeter and perimeter to area ratio than wild-type cells (Fig. 3B′,C′,B″,C″; Fig. S3D,F). We also observe that in SqhA21 embryos, cells are more elongated in the medio-lateral (ML) axis than wild-type cells are (Fig. 3A‴), suggesting that these cells are being stretched more in this axis as a result of the resistance of the epidermis. Altogether, these observations provide evidence for a role of Myosin in apical area and membrane contraction in AS cells.

Since in SqhA21 and SqhE21 embryos the contraction of AS cells is affected, we analysed if this perturbed cell behaviour also affected tissue closure. The contractile force of the AS is the major force driving epidermal closure, but previous mechanical-jump experiments have shown that when one process is defective, others can compensate (Hutson et al., 2003). Hence, it is possible that cellular defects did not result in tissue closure defects. Previous work has shown that AS cells contract mostly in the dorso-ventral axis, with only a minor and late contribution of contraction in the antero-posterior axis (Gorfinkiel et al., 2009; Kiehart et al., 2000). Thus, a way to assess the contraction of the AS driven by the contraction of AS cells is by examining the evolution of the ML axis of the ellipse formed by the AS tissue (Fig. 3D). We observe that the ML length of the AS at its symmetry axis is smaller in embryos carrying a phosphomimetic form of Sqh and larger in embryos carrying the non-phosphorylatable form (Fig. 3E). Moreover, the proportional rate of change in ML length of the AS ellipse is higher in SqhE21 embryos, showing that Myosin activity produces not only a smaller tissue but also a tissue that contracts faster (Fig. 3F). In contrast, there is no decrease in the proportional rate of change of the ML axis in SqhA21 embryos. We interpret this as being a consequence of the robustness of DC and that other processes are compensating for a defective AS cell contraction.

Myosin is activated by Rok in AS cells

Our results suggest that the control of Myosin phosphorylation is important for the dynamics of apical cell oscillations and apical contraction. In other tissues with oscillatory activity, Myosin phosphorylation is controlled by Rok and Mbs (Dawes-Hoang et al., 2005; He et al., 2010; Kasza et al., 2014; Mason et al., 2013; Munjal et al., 2015; Valencia-Expósito et al., 2016; Vasquez et al., 2014). In AS cells, a kinase-dead (SqhRokK116A::GFP) Rok reporter (or a wild-type Rok reporter in a rok^2 mutant background) localizes at medioapical foci and also at the level of the cell membranes (Fig. 4A and Movies 4,5). To analyse if the activity of Rok regulates Myosin localization in AS cells, we injected DE-Cadherin::mTomato, Sqh::GFP DC embryos with the Rok inhibitor Y-27632. In these embryos, both cell area and Myosin oscillations are strongly attenuated, showing that in AS cells Rok also controls Myosin activity (Fig. 4C-D″; Movie 6). Conversely, we observed that the ectopic expression of a constitutive active form of Rok in the AS produces a premature contraction of cells (data not shown).

Antibody staining of DC embryos shows that Mbs is present in the AS (Fig. S1C) and live imaging of an Mbs::GFP reporter (Sen et al., 2012) shows that it localizes in medioapical foci (Fig. 4B; Movie 7). These observations show that in AS cells, both Rok and Mbs localize in medioapical foci, as shown in other cells with oscillatory dynamics (Munjal et al., 2015) and point to a universal mechanism for the emergence of the oscillatory actomyosin activity.

Mbs is required for AS tissue integrity

We next investigated the role of Mbs. First, we ectopically expressed a constitutive active form of Mbs (MbsN300) in AS cells (Fig. 5A-A″; Movie 8) and measured the dynamics of Myosin foci, which showed an increased cycle length, similar to SqhA21 foci (Fig. 5C-E). Interestingly, only very few MbsN300 cells

Development (2016) 143, 4676-4686 doi:10.1242/dev.136127

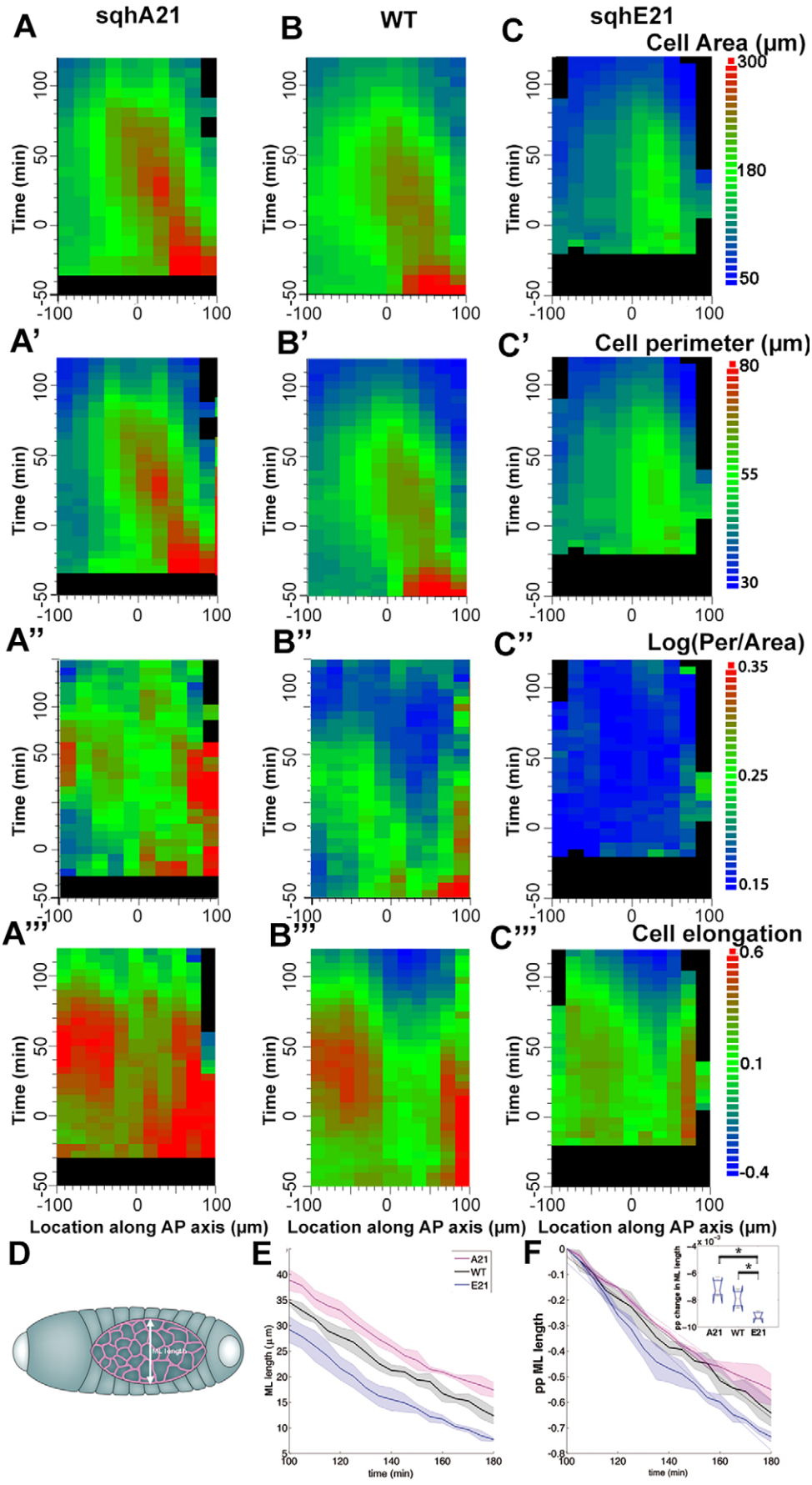

Fig. 3. Cell geometry and tissue closure in Sqh phosphomutants. Apical cell area (A-C), cell perimeter (A′-C′), log ratio of cell perimeter to cell area (A″-C″) and cell shape ML elongation (A‴-C‴) of AS cells from SqhA21 (A-A‴), wild-type (B-B‴) and SqhE21 (C-C‴) embryos as a function of their AP location over time. (D) Schematic representation of the AS indicating the minor axis of the ellipse or ML length. (E) ML length from 100 min onwards of the AS of the different phosphomutants. (F) Proportional ML length from 100 min onwards. Data plotted are the mean ML lengths pooled from three embryos per genotype. Ribbons represent s.d. Inset in F shows a box plot of the rate of change in proportional ML length. **P*<0.05 (Student's *t*-test). ML length was measured from 100 min onwards as then the AS was in the whole field of view for the three different genotypes.

Development (2016) 143, 4676-4686 doi:10.1242/dev.136127

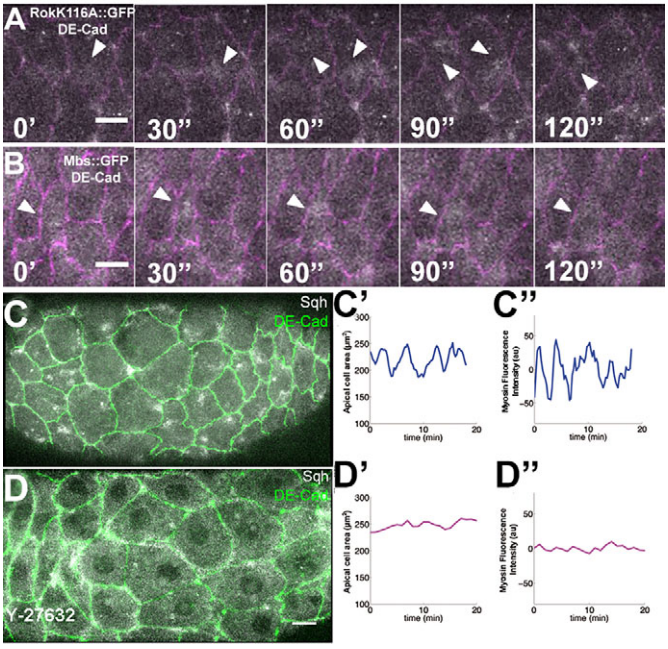

Fig. 4. Regulation of Myosin localization by Rok. (A) Still images from a time-lapse movie of an example DC DE-Cadherin::mTomato, *sqh*-RokK116G::GFP embryo. (B) Still images from a time-lapse movie of an example DC C381Gal4, DE-CadGFP; UAS-Mbs::GFP/+ embryo. Arrowheads indicate foci. (C) Still image from a time-lapse movie of an example wild-type DC DE-Cadherin::mTomato, Sqh::GFP embryo. Apical cell area (C′) and Myosin fluorescence intensity over time (C″) of an example cell. (D) Still image from a time-lapse movie of a DE-Cadherin-mTomato, Sqh::GFP embryo incubated with the Rok inhibitor Y-27632 at 1 mM. Apical cell area (D′) and Myosin fluorescence intensity over time (D″) of an example cell. Fifteen cells of 3 embryos injected with 1 mM Y-27632 and 10 cells of 2 control embryos injected with water were analysed. Scale bars: 10 µm.

exhibited discernible cell shape oscillations (Fig. S4A,B), which prevented us from measuring their amplitude and period. Thus, this result shows that the low levels of Myosin activity remaining in these embryos are not enough to drive cell shape oscillations. As a consequence, apical cell area, perimeter, ratio of perimeter to area, and ML elongation of AS cells are all greater than in wild-type embryos (Fig. S4F-M), showing that these cells cannot contract properly. In spite of this, the tissue contracts and DC is completed, suggesting that other forces can compensate the defective apical contraction of AS cells (Hutson et al., 2003).

We then analysed the effect of reducing Mbs activity. It has been shown that *mbs* mutant embryos have DC defects, evident in the lack of elongation of dorsal epidermal cells and in adhesion defects between the epidermis and the AS (Mizuno et al., 2002; Tan et al., 2003). To analyse whether *mbs* had a function in the AS, we decided to revisit the phenotypes of these embryos and performed time-lapse movies of zygotic DE-Cadherin::GFP, mbs^{541} mutant embryos during the whole process of DC (Fig. 5B-B″; Movie 9). At the beginning of the process, the AS looks normal and starts contracting in a timely manner. However, as DC proceeds and usually after the zippering has engaged, we observe tears between the epidermis and the AS, but also within the AS, giving rise to a loss of integrity of the tissue (Fig. 5B′,B″ and Movie 9).

To analyse if these tears resulted from an increase in Myosin activity, we measured several parameters used in this work that were found to be associated with the levels of Myosin activity. In mbs^{541} mutant embryos, the cycle length of Myosin foci decreases, and this is due to a decrease both in the duration and the time interval between foci, similar to what happens in SqhE21::GFP embryos. However, Myosin persistence is not significantly different from the wild type (data not shown), nor is the period and amplitude of oscillations, the apical area, the apical perimeter or the ML elongation of AS cells (Fig. 5G,H; Fig. S4C-D,F′-M′). These results suggest that Myosin foci dynamics in mbs^{541} mutant embryos is not as affected as in SqhE21 embryos.

The ectopic expression of a constitutive active form of Myosin light chain kinase induces precocious contraction of AS cells but no tears (Fischer et al., 2014), suggesting that an increase in Myosin activity cannot be the only factor contributing to the appearance of tears within the AS of mbs^{541} mutant embryos. We noticed that the tears within the AS usually appear at sites of cell delamination. It is known that around 10% of AS cells are eliminated from the epithelium through a mechanism involving cytoskeletal rearrangements in the delaminating cell and also in its nearest neighbours (Meghana et al., 2011; Muliyil et al., 2011; Toyama et al., 2008). We observe that the number of cell delamination events in mbs^{541} mutant embryos increases, but this is not due to an increase in cell density (Fig. 5F,F′). We thus analysed whether tears in mbs^{541} embryos were associated with changes in Myosin localization. Time-lapse movies of the AS of late DC embryos show that in wild-type embryos, cells surrounding the delaminating cell exhibit dynamic Myosin foci during and after the delamination process (Fig. 6A,A′). In contrast, in mbs^{541} mutant embryos, once a cell is delaminated, surrounding cells show an accumulation of Myosin at the level of the membranes (Fig. 6B,C). This aberrant Myosin localization is evident after the cell delamination has occurred, suggesting that it might be a response of the cells to the tears generated by a defective delamination process.

Adhesion defects in *mbs* mutant embryos

Delamination events from the plane of the epithelium, also called T2 processes, involve junction removal between the extruded cell and its neighbours, and the formation and maintenance of a new interface between cells to maintain the integrity of the tissue (Guillot and Lecuit, 2013) (Fig. 6G). We observe defects in these processes in mbs^{541} embryos. In 7% of the T2 processes analysed, junctions between the extruding cells and its neighbours do not complete shrinkage (Fig. 6E) and show a decrease in DE-Cadherin fluorescence levels (Fig. 6H). In 39% of cases, junction removal was completed, but a new interface between new neighbours was not properly formed (Fig. 6F). These observations suggest that DE-Cadherin-mediated adhesion could be affected in mbs^{541} mutant embryos. In support of this, we find that an increase in the levels of DE-Cadherin with the ubi-DE-Cadherin::GFP transgene rescued the integrity of the AS tissue of mbs^{541} mutant embryos (Fig. 6I,I′). We also found that DE-Cadherin fluorescence intensity levels at the level of interfaces tend to be lower in mbs^{541} mutant embryos than in embryos expressing MbsN300, suggesting that Mbs stabilizes DE-Cadherin at the cell membrane (Fig. S4N-P).

Mbs has been shown to regulate not only Myosin phosphorylation but also Moesin (Fukata et al., 1998), an ERM (Ezrin, Radixin, Moesin) protein linking the actin cytoskeleton to transmembrane proteins that has been involved in maintaining epithelial integrity (Fehon et al., 2010). Thus, we investigated whether misregulation of Moesin could be contributing to the appearance of tears in the AS of mbs^{541} mutant embryos. An antibody against the phosphorylated form of Moesin (P-Moe) shows that it localizes to cell-cell junctions of stage 13 AS cells, but there is also general staining in the medioapical region (Fig. 7A-A″).

Development (2016) 143, 4676-4686 doi:10.1242/dev.136127

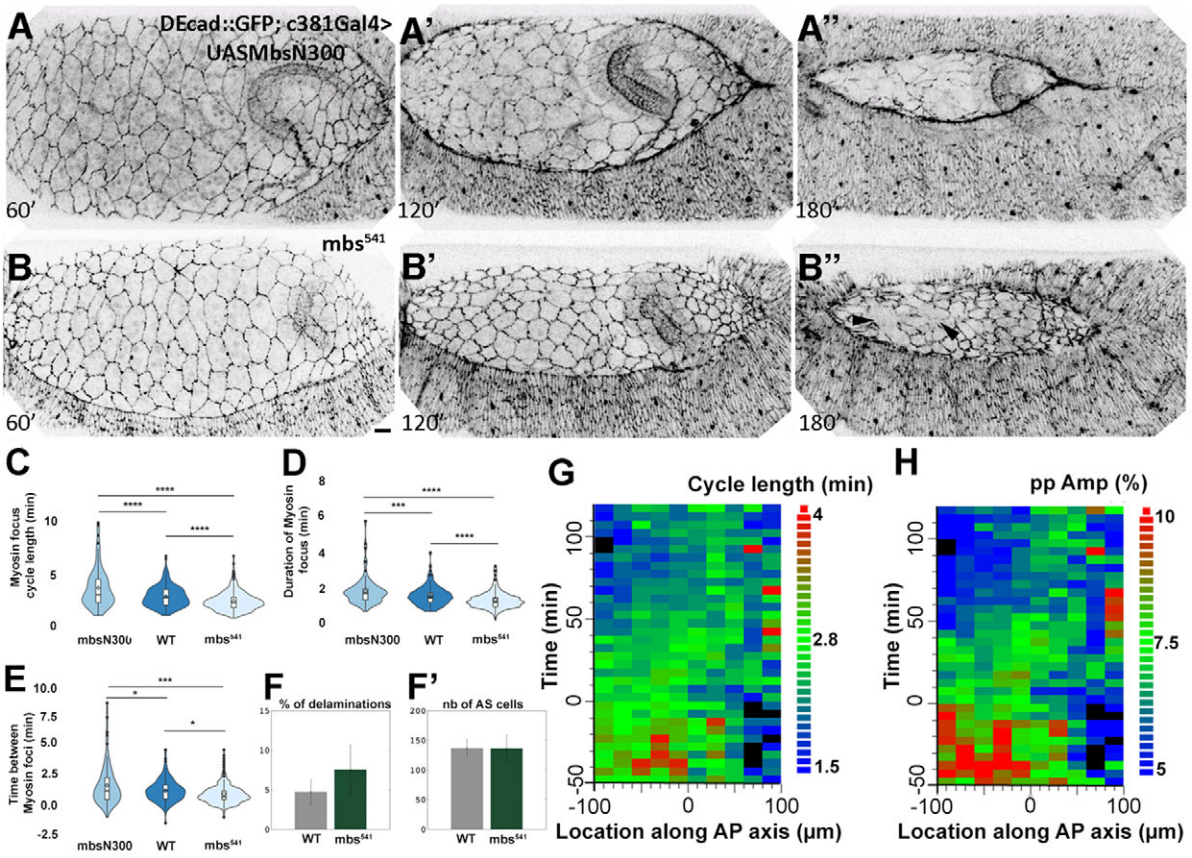

Fig. 5. Myosin foci dynamics and cell shape fluctuations in embryos with perturbed Mbs activity. (A-B″) Still images from a time-lapse movie of example DE-Cadherin::GFP,c381Gal4/UASMbsN300 (A-A″) and DE-Cadherin::GFP, *mbs*^{541} (B-B″) mutant embryos at 60, 120 and 180 min of DC. Arrowheads in B″ indicate sites of tears within the AS tissue. Out of 16 *mbs*^{541} mutant embryos analysed, 7 showed tears within the AS tissue before detachments between the AS and the epidermis were visible, 5 showed the appearance of tears within the AS and between the two tissues almost simultaneously, 2 had detachments between the AS and the epidermis before tears in the AS appeared, and 2 did not show any obvious DC defects. (C) Cycle length, (D) duration and (E) time interval of Myosin foci. Eleven cells from 3 ubi-DE-Cadherin::GFP,zipper::YFP; c381Gal4>UASMbsN300 embryos, 28 cells from 5 *mbs*^{541} mutant embryos and 23 cells from 6 wild-type embryos were analysed and foci duration and time interval between foci was computed manually over 25 min. See also Table S1. **P*<0.05, ***P*<0.01, ****P*<0.001, *****P*<0.0001; NS, not significant (Mann–Whitney test). (F) Percentage of cell delaminations and (F′) number of AS cells at the onset of DC in 7 wild-type and 5 *mbs*^{541} embryos. (G) Mean cycle length and (H) proportional amplitude of AS cell shape oscillations from 5 *mbs*^{541} mutant embryos as a function of their AP location over time. Average of 47 cells per embryo were sampled every 30 s. Scale bar: 10 µm.

In late DC embryos, however, P-Moe is not seen localizing to apical cell membranes but shows a general punctuated localization throughout the whole apical region of the cell (Fig. 7B-B″). To analyse if Mbs regulates Moesin phosphorylation, we ectopically expressed the constitutive active form of Mbs (MbsN300) with the prd-GAL4 driver (expressed in alternate stripes). Sqh phosphorylation (Sqh-1P) levels are reduced in alternate stripes both in the epidermis and the AS, showing that Mbs can indeed regulate phosphorylation of this protein (Fig. 7D,E). Interestingly, we also observe a decrease of P-Moe signal at cell membranes, and this decrease is specific to the AS (Fig. 7C-C‴).

These results raised the possibility that an increase in the levels of phosphorylated Moesin could be underlying the loss of integrity of the AS from *mbs*^{541} mutant embryos. Thus, we ectopically expressed a phosphomimetic (MoeT559D) or a non-phosphorylatable (MoeT559A) form of Moesin (Speck et al., 2003) in the AS of *mbs*^{541} mutant embryos. With the ectopic expression of MoeT559D, tears between the AS and the epidermis and within the AS are observed, giving rise to an AS that loses its integrity in most of the embryos (Fig. 7F′, Movie 9). In contrast, in *mbs*^{541} mutant embryos in which MoeT559A is ectopically expressed in the AS, we never observed tears between the AS and the epidermis and embryos reached late DC stages with no tears within the AS (Fig. 7F, Movie 9). Analysis of cuticles laid by these embryos confirms a rescue of DC defects in embryos in which MoeT559A was expressed (Fig. 7F″), supporting the idea that the DC defects of *mbs*^{541} mutant embryos are due, at least in part, to a misregulation of Moesin phosphorylation.

DISCUSSION

Integrating temporal and spatial scales in tissue morphogenesis

In this work, we have analysed the contribution of Myosin activity to Myosin foci dynamics, cell oscillations, cell shape changes and AS contraction. Although we cannot rule out that the defects we observe at any of these scales could be due to defects in the supra-cellular actomyosin cable formed at the interface between the AS and the epidermis, we think that the observed defects are much better explained by a direct role of Myosin foci in AS cell and AS tissue behaviour.

Our results show that there is a correlation between increasing Myosin activity and decreasing cycle length of Myosin foci, and further show that this is mostly because the frequency of foci increases, giving rise to an increase in Myosin persistence (Fig. 8).

Development (2016) 143, 4676-4686 doi:10.1242/dev.136127

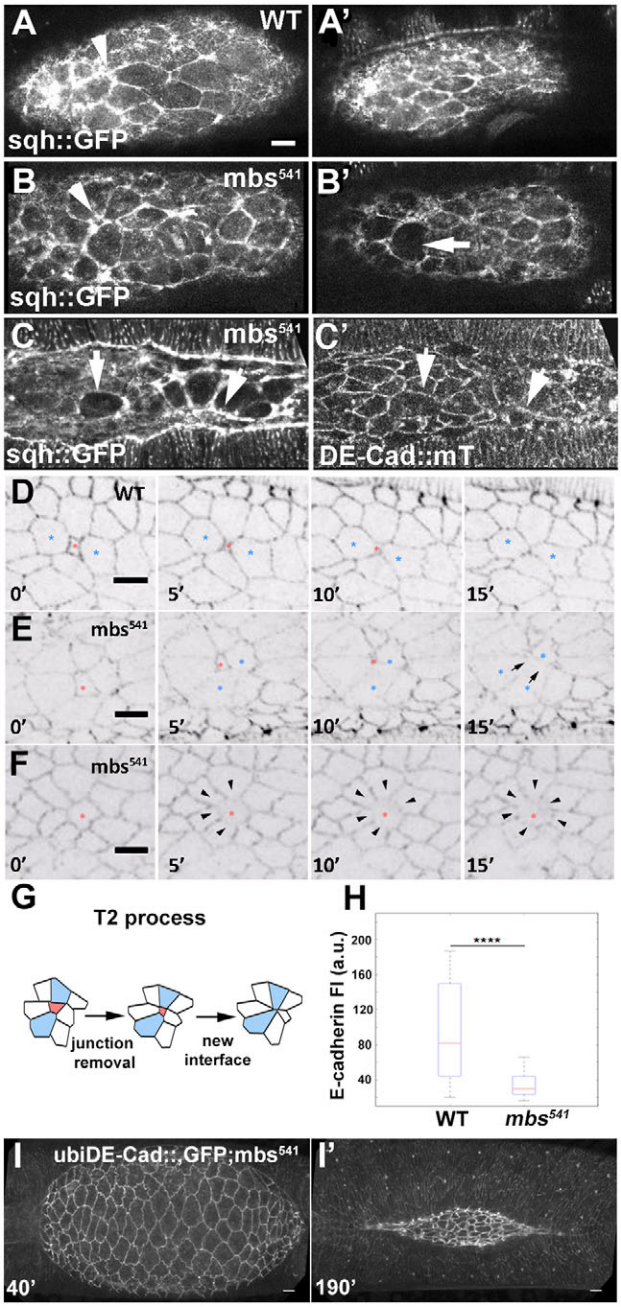

Fig. 6. Adhesion defects in *mbs*^{541} mutant embryos. (A-C′) Localization of Sqh::GFP during cell delamination in wild-type DE-Cadherin::mTomato, Sqh::GFP (A,A′) and *mbs*^{541} mutant (B-C′) embryos at the end of the cell delamination process (A,B, arrowheads) and after 30 min (A′,B′). Note the loss of medioapical Sqh (B′, arrow) and the accumulation of junctional Sqh (C,C′, arrows) in cells surrounding the delaminating cell in *mbs*^{541} mutant embryo. (D-F) Still images from a time-lapse movie of wild-type (D) and DE-Cadherin::GFP, *mbs*^{541} mutant embryos (E,F) during a cell delamination event. The starting point of a delamination event is the time point at which the area of the extruded cell is 60-80% of its neighbours' area. In wild-type embryos, of 74 cell delamination events analysed (7 embryos), 60 formed a new interface between new neighbours after the T2 process was completed and 14 stayed as a four-way vertex. In *mbs*^{541} embryos, of 127 cell delamination events analysed (7 embryos), 53 showed a defect in the formation and maintenance of the new interface (E) and 9 showed a defect at interfaces between the delaminating cell and its neighbours (F). The delaminating cell is marked with a red asterisk and 2 neighbouring cells are marked with a blue asterisk. Note the loss of DE-Cadherin of the interfaces between the delaminating cells and its neighbours in *mbs*^{541} mutants (F, arrowheads), or the absence of a new junction after a cell has been delaminated (E, arrowhead). (G) Cartoon illustrating a T2 process involving the removal of junctions between the extruding cell and its neighbours and the formation and maintenance of a new interface. (H) DE-cadherin fluorescence intensity at the interfaces between a delaminating cell and its neighbours. Forty interfaces of 4 wild-type embryos and 42 interfaces of 4 *mbs*^{541} mutant embryos in which the delamination process was not completed (F) were used to measure DE-Cadherin fluorescence levels when the delaminating cell was 60-80% of its neighbour's area. (I,I′) Rescue of AS integrity in ubi-DE-Cadherin::GFP, *mbs*^{541} mutant embryos (11 out of 12 embryos closed without tears). Scale bars: 10 µm.

An increase in the persistence of medioapical Myosin in phosphomimetic Sqh mutants has also been observed in ventral cells undergoing gastrulation (Vasquez et al., 2014). In germ-band cells, Sqh phosphomimetic mutants show greater pulse duration and amplitude (Munjal et al., 2015), also suggesting more-persistent contractile networks. In the follicular epithelium, where actomyosin oscillations occur at the basal side of the cells, an increase in the levels of phosphorylated Myosin produces Myosin pulses that are more asynchronic (Valencia-Expósito et al., 2016) but the duration or persistence of these Myosin pulses has not been reported. Whether the duration and frequency of Myosin pulses in the different cell types depends on the time-scale of fluctuations or other cell features, remains to be investigated. Several theoretical models have been proposed to explain the mechanisms underlying actomyosin and cell oscillations (Gorfinkiel, 2016; Valencia-Expósito et al., 2016). It would be very interesting if a unifying quantitative framework were able to account for the differences observed in the different systems.

In AS cells, increased Myosin persistence gives rise to an increase in the contraction period of the oscillation cycle and in the amplitude of cell area oscillations, producing more contracted cells. Conversely, low Myosin activity as observed with the ectopic expression of MbsN300, attenuates oscillations and gives rise to poorly contracting cells. Thus, our results show a relationship between the oscillatory behaviour of AS cells and their contractility. Moreover, we propose that it is not the absolute frequency of cell area oscillations that determines the contractile state of AS cells but the relative durations of the expansion relative to contraction phases. In wild-type embryos, apical cell oscillations become more symmetric (Blanchard et al., 2010) and Myosin foci become more frequent and more persistent (David et al., 2013; Machado et al., 2015) as DC progresses. Thus, our results suggest that the evolution in Myosin dynamics and cell shape oscillations as DC progresses could be driven by an increase in Myosin phosphorylation.

At the cellular level, we observe that the contraction of the apical surface area and cell membranes is coupled. It is not clear how Myosin activity drives membrane shrinkage in wild-type AS cells. It is possible that, similar to what happens in the germ-band, medial Myosin foci promote apical membrane shrinkage through polarized Myosin flow towards the junctions (Rauzi et al., 2010), inducing the accumulation of Myosin at the level of junctions.

Mbs as coordinator of cytoskeletal activity and adhesion

As shown in other systems, both Rok and Mbs colocalize with Myosin to medioapical pulses (this work and data not shown) providing evidence that they regulate Myosin pulsatile dynamics. We further find that in *mbs* mutant embryos, the AS tears apart at sites of cell delamination. Although the number of cells delaminating from the plane of the epithelium is increased in these mutants, an increase in cell delamination events by other

Development (2016) 143, 4676-4686 doi:10.1242/dev.136127

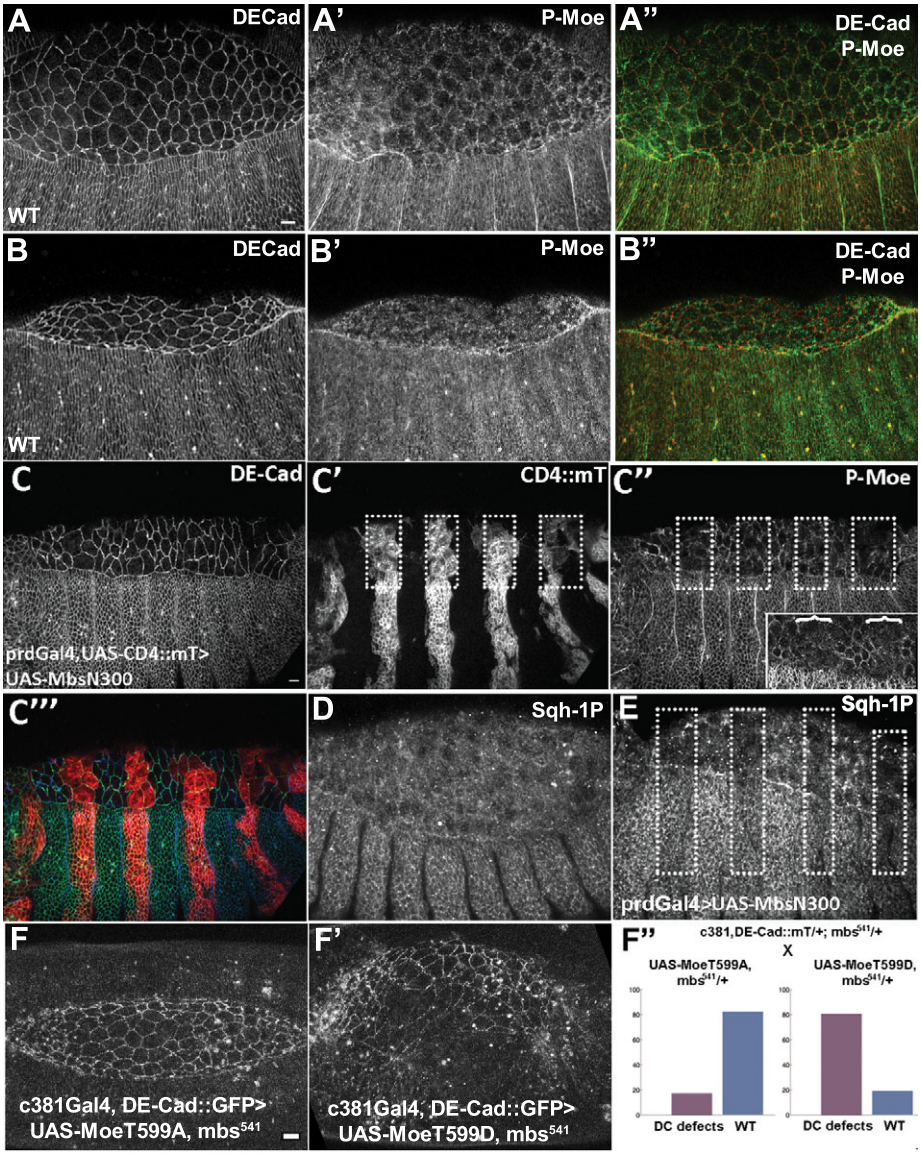

Fig. 7. Mbs function in the AS is mediated by Moesin. (A-B″) Stage 13 (A-A″) and stage 14 (B-B″) embryos stained for DE-Cadherin (A,B) and phosphorylated Moesin (A′,B′). (A″,B″) Merged channels. (C-E) Stage 13 prd-GAL4>UAS-MbsN300 embryos stained for DE-Cadherin (C) and phosphorylated Moesin (C″). Inset in C″ shows magnification of a different embryo. (C′) CD4::mT signal. (C‴) Merge of the three channels. Stage 13 wild-type embryo (D) and stage 13 prd-GAL4>UAS-MbsN300 embryo (E) stained for monophosphorylated Sqh (Sqh-1P). Dotted boxes (C′,C″,E) and brackets (C″, inset) indicate the regions where MbsN300 is expressed and where P-Moe levels decrease. (F,F′) Still images of example embryos with ectopic expression of MoeT559A (F) and MoeT559D (F′) in the AS of *mbs*^{541} mutants. (F″) Percentage of DC defects in cuticles from the indicated genotypes. DC defects include cuticles with antero-dorsal holes, and cuticles with anterior holes and dorsal puckering. WT cuticles include apparently wild-type cuticles and cuticles with only mouth hook defects. Bar plots represent mean values of the data. Scale bar: 10 µm.

means does not cause a loss of integrity of the tissue (Muliyil et al., 2011; Muliyil and Narasimha, 2014; Toyama et al., 2008), suggesting that cell delamination events per se do not generate tears. Instead, our results suggest that an imbalance in contractility and/or adhesion could also contribute to trigger cell delaminations.

We observe that the loss of integrity of the AS in *mbs* mutant embryos is due to defective DE-Cadherin junction remodelling. We do not know how Mbs regulates DE-Cadherin dynamics, but it may involve Moesin function. Consistent with our results that an increase in the levels of phosphorylated Moesin could prevent proper junction remodelling in *mbs* mutant embryos, is the observation that increased apical Moesin activity prevents cell shape changes during the morphogenesis of salivary glands (Xu et al., 2011). Thus, our results suggest that the levels of phosphorylated Moesin must be tightly controlled to allow for the rapid cell shape changes AS cells are undergoing during late DC. Mbs dephosphorylates Moesin in the AS and not in the epidermis, suggesting that this is a tissue-specific effect. Interestingly, it has recently been reported that an AS-specific function of Crumbs involving its FERM binding domain also affects actomyosin contractility and adhesion in this tissue (Flores-Benitez and Knust, 2015). In that work, a phosphomimetic form of Moesin was able to rescue the defects caused by this particular Crumbs mutant. This result is in principle at odds with our observations. However, the defects in the AS of Crumbs mutants were observed as early as germ-band retraction stages. Thus, it is possible that the requirements for junction dynamics change during late DC, which is not surprising given that, by this stage, cells have to contract quickly and rapidly remodel their junctions. Moreover, in the epithelium of imaginal discs, it has been found that the ectopic expression of both a phosphomimetic and a non-phosphorylatable form of Moesin induces loss of tissue integrity and apoptosis (Yang et al., 2012), suggesting that it is not simply the absence of Moesin that is detrimental for epithelial homeostasis but its misregulation.

An interplay between myosin contractility, actin dynamics and E-Cadherin recruitment has been observed in cultured suspended cells (Engl et al., 2014). Myosin contractility affects actin turnover, which, in turn, regulates E-Cadherin recruitment, providing mechano-sensitive regulation of adhesion strength. Thus, a possible scenario is that in *mbs* mutant embryos, changes in both Myosin contractility and Moesin-dependent actin dynamics lead to

Development (2016) 143, 4676-4686 doi:10.1242/dev.136127

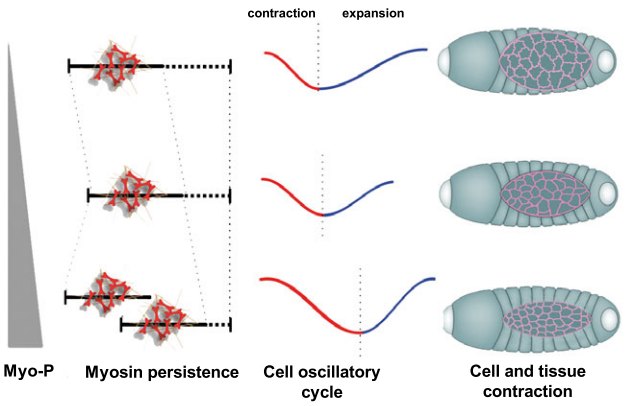

Fig. 8. The correlation between Myosin activity, actomyosin foci dynamics, the shape of the cell oscillatory cycle and the contraction of AS cells and tissue. The levels of Myosin activity influence the frequency of Myosin foci formation. As the levels of Myosin activity increase, there is an increase in the persistence of Myosin at the apical cortex of the cells. This gives rise to an increase in the duration of the contraction half-cycle relative to the expansion half-cycle of the oscillatory cycle of amnioserosa cells. At the cellular level, the effect is an increase in the contractile state of the cells, generating a more contractile tissue.

defective DE-Cadherin recruitment and produce the loss of integrity of the tissue.

MATERIALS AND METHODS

Fly stocks and genetics

For a complete list of stocks used in this work, see the supplementary Materials and Methods.

Live-imaging

Stage 12-13 *Drosophila* embryos were dechorionated, mounted in coverslips with the dorsal side glued to the glass and covered with Voltalef oil 10S (Attachem). The AS was imaged at 25-28°C using an inverted LSM 710 Meta laser-scanning microscope with a 40× or a 63× oil immersion Plan-Fluor (NA=1.3) objective. GFP and mTomato cytoskeletal reporters were simultaneously imaged with an argon laser and a 651 nm diode laser. For whole AS imaging, 15-16 *z*-sections were collected 1.5 µm apart every 30 s. For cytoskeletal dynamics imaging, 5-6 *z*-sections 1 µm apart were collected every 10-15 s.

Image analysis and statistics

The morphometric analysis of AS cells and fluctuations was carried out as described in the supplementary Materials and Methods using automated tracking of the AS cell shapes with custom software written in Interactive data language (IDL, Exelis), as described previously (Blanchard et al., 2009, 2010). Statistical analysis was carried out as detailed in the supplementary Materials and Methods.

Myosin foci dynamics and statistics

Myosin foci dynamics was computed manually from time-lapse images with 15 s time intervals, which allowed us to follow the assembly and disassembly of each focus in an accurate manner. Central cells of the AS were chosen to quantify Myosin dynamics. The times associated with the duration of foci were obtained by counting the number of frames since a Myosin focus was visible until its signal was lost. The times associated with the time interval between consecutive foci were obtained by counting the number of frames in which no apicomedial Myosin signal was detected. Statistical analysis of Myosin foci dynamics was done considering each Sqh::GFP focus as an individual event, computing the duration and time interval of each focus individually. In embryos in which MbsN300 was ectopically expressed, we measured the dynamics of Myosin foci using the zipper::YFP reporter (we reasoned that using the *sqh::GFP* transgene – which is under the control of its own promoter – could lead to a partial rescue of the MbsN300 phenotype), whose dynamics has been found to be statistically indistinguishable from Sqh::GFP dynamics (David et al., 2010). Pooled data of these variables was then compared between genotypes using a Mann–Whitney *U*-test since they did not follow a standard normal distribution, previously tested with a one-sample Kolmogorov–Smirnov test (Statistics ToolBox of MATLAB).

Drug injections

Embryos were prepared as for live-imaging and injected posteriorly in the peri-vitelline space with the drug inhibitor Y-27632 (Enzo Life Sciences) at 1 mM in water. Embryos were imaged immediately as indicated in the live-imaging section. Higher concentrations gave rise to a complete disorganization of the AS tissue, while lower concentrations did not produce discernible effects.

Immunostaining

Embryos were fixed and stained as previously described (Kaltschmidt et al., 2002). The following primary antibodies were used: rat monoclonal against DE-Cadherin (DCAD2, Developmental Studies Hybridoma Bank; 1:50), Guinea pig against the monophosphorylated form of Sqh at Ser21 [a gift from Robert E. Ward (Zhang and Ward, 2011); 1:500], rabbit against phospho-Moesin (Cell Signaling, 3141; 1:100). Alexa 488, Alexa 647 and Jackson Cy5-conjugated antibodies from Molecular Probes were used as secondary antibodies.

Cuticle preparations

Embryos were collected from 24-h-old eggs and then aged for 48 h at 25°C. They were dechorionated in bleach and mounted with the vitelline membrane in acetic acid-Hoyers (1:1) and the slide was incubated overnight at 65°C.

Acknowledgements

We are very grateful to Guy B. Blanchard for the development of oTracks software, discussions and critical reading of the manuscript. We thank Adam Martin, Jessica Treisman, Change Tan, Michael Krahn, Jennifer Zallen, Guy Tanentzapf and Bloomington Stock Centre for *Drosophila* strains. We thank Eva Caminero for drug injections, Change Tan for the MYPT antibody and Robert Ward for the Sqh antibodies.

Competing interests

The authors declare no competing or financial interests.

Author contributions

N.G. conceived the project. J.D. and N.G. performed the experiments, analysed the data and discussed the results. N.G. wrote the paper.

Funding

This work was supported by grants from the Ministerio de Ciencia e Innovación (BFU-2011-25828 and 'Ramón y Cajal' fellowship award) and a European Commission Marie Curie Career Integration Grant (PCIG09-GA-2011-293479). J.D. is a recipient of a PhD FPI-fellowship (BES-2012-051839) from the Ministerio de Ciencia e Innovación.

Supplementary information

Supplementary information available online at
http://dev.biologists.org/lookup/doi/10.1242/dev.136127.supplemental

References

Azevedo, D., Antunes, M., Prag, S., Ma, X., Hacker, U., Brodland, G. W., Hutson, M. S., Solon, J. and Jacinto, A. (2011). DRhoGEF2 regulates cellular tension and cell pulsations in the amnioserosa during Drosophila dorsal closure. *PLoS ONE* **6**, e23964.

Blanchard, G. B., Kabla, A. J., Schultz, N. L., Butler, L. C., Sanson, B., Gorfinkiel, N., Mahadevan, L. and Adams, R. J. (2009). Tissue tectonics: morphogenetic strain rates, cell shape change and intercalation. *Nat. Methods* **6**, 458-464.

Blanchard, G. B., Murugesu, S., Adams, R. J., Martinez-Arias, A. and Gorfinkiel, N. (2010). Cytoskeletal dynamics and supracellular organisation of cell shape fluctuations during dorsal closure. *Development* **137**, 2743-2752.

David, D. J. V., Tishkina, A. and Harris, T. J. C. (2010). The PAR complex regulates pulsed actomyosin contractions during amnioserosa apical constriction in Drosophila. *Development* **137**, 1645-1655.

David, D. J. V., Wang, Q., Feng, J. J. and Harris, T. J. C. (2013). Bazooka inhibits aPKC to limit antagonism of actomyosin networks during amnioserosa apical constriction. *Development* **140**, 4719-4729.
Dawes-Hoang, R. E., Parmar, K. M., Christiansen, A. E., Phelps, C. B., Brand, A. H. and Wieschaus, E. F. (2005). *folded gastrulation*, cell shape change and the control of myosin localization. *Development* **132**, 4165-4178.
Engl, W., Arasi, B., Yap, L. L., Thiery, J. P. and Viasnoff, V. (2014). Actin dynamics modulate mechanosensitive immobilization of E-cadherin at adherens junctions. *Nat. Cell Biol.* **16**, 587-594.
Fehon, R. G., McClatchey, A. I. and Bretscher, A. (2010). Organizing the cell cortex: the role of ERM proteins. *Nat. Rev. Mol. Cell Biol.* **11**, 276-287.
Fischer, S. C., Blanchard, G. B., Duque, J., Adams, R. J., Arias, A. M., Guest, S. D. and Gorfinkiel, N. (2014). Contractile and mechanical properties of epithelia with perturbed actomyosin dynamics. *PLoS ONE* **9**, e95695.
Flores-Benitez, D. and Knust, E. (2015). Crumbs is an essential regulator of cytoskeletal dynamics and cell-cell adhesion during dorsal closure in *Drosophila*. *eLife* **4**, 5984.
Fukata, Y., Kimura, K., Oshiro, N., Saya, H., Matsuura, Y. and Kaibuchi, K. (1998). Association of the myosin-binding subunit of myosin phosphatase and moesin: dual regulation of moesin phosphorylation by Rho-associated kinase and myosin phosphatase. *J. Cell Biol.* **141**, 409-418.
Gorfinkiel, N. (2016). From actomyosin oscillations to tissue-level deformations. *Dev. Dyn.* **245**, 268-275.
Gorfinkiel, N. and Blanchard, G. B. (2011). Dynamics of actomyosin contractile activity during epithelial morphogenesis. *Curr. Opin. Cell Biol.* **23**, 531-539.
Gorfinkiel, N., Blanchard, G. B., Adams, R. J. and Martinez Arias, A. (2009). Mechanical control of global cell behaviour during dorsal closure in Drosophila. *Development* **136**, 1889-1898.
Guillot, C. and Lecuit, T. (2013). Mechanics of epithelial tissue homeostasis and morphogenesis. *Science* **340**, 1185-1189.
He, L., Wang, X., Tang, H. L. and Montell, D. J. (2010). Tissue elongation requires oscillating contractions of a basal actomyosin network. *Nat. Cell Biol.* **12**, 1133-1142.
Heissler, S. M. and Sellers, J. R. (2015). Myosin light chains: teaching old dogs new tricks. *Bioarchitecture* **4**, 169-188.
Hutson, M. S., Tokutake, Y., Chang, M.-S., Bloor, J. W., Venakides, S., Kiehart, D. P. and Edwards, G. S. (2003). Forces for morphogenesis investigated with laser microsurgery and quantitative modeling. *Science* **300**, 145-149.
Jordan, P. and Karess, R. (1997). Myosin light chain–activating phosphorylation sites are required for oogenesis in Drosophila. *J. Cell Biol.* **139**, 1805-1819.
Kaltschmidt, J. A., Lawrence, N., Morel, V., Balayo, T., Fernandez, B. G., Pelissier, A., Jacinto, A. and Martinez-Arias, A. (2002). Planar polarity and actin dynamics in the epidermis of Drosophila. *Nat. Cell Biol.* **4**, 937-944.
Kasza, K. E., Farrell, D. L. and Zallen, J. A. (2014). Spatiotemporal control of epithelial remodeling by regulated myosin phosphorylation. *Proc. Natl. Acad. Sci. USA* **111**, 11732-11737.
Kiehart, D. P., Galbraith, C. G., Edwards, K. A., Rickoll, W. L. and Montague, R. A. (2000). Multiple forces contribute to cell sheet morphogenesis for dorsal closure in Drosophila. *J. Cell Biol.* **149**, 471-490.
Lecuit, T. and Yap, A. S. (2015). E-cadherin junctions as active mechanical integrators in tissue dynamics. *Nat. Cell Biol.* **17**, 533-539.
Machado, P. F., Duque, J., Étienne, J., Martinez-Arias, A., Blanchard, G. B. and Gorfinkiel, N. (2015). Emergent material properties of developing epithelial tissues. *BMC Biol.* **13**, 98.
Mason, F. M., Tworoger, M. and Martin, A. C. (2013). Apical domain polarization localizes actin–myosin activity to drive ratchet-like apical constriction. *Nat. Cell Biol.* **15**, 926-936.
Meghana, C., Ramdas, N., Hameed, F. M., Rao, M., Shivashankar, G. V. and Narasimha, M. (2011). Integrin adhesion drives the emergent polarization of active cytoskeletal stresses to pattern cell delamination. *Proc. Natl. Acad. Sci. USA* **108**, 9107-9112.
Mizuno, T., Tsutsui, K. and Nishida, Y. (2002). Drosophila myosin phosphatase and its role in dorsal closure. *Development* **129**, 1215-1223.
Muliyil, S. and Narasimha, M. (2014). Mitochondrial ROS regulates cytoskeletal and mitochondrial remodeling to tune cell and tissue dynamics in a model for wound healing. *Dev. Cell* **28**, 239-252.
Muliyil, S., Krishnakumar, P. and Narasimha, M. (2011). Spatial, temporal and molecular hierarchies in the link between death, delamination and dorsal closure. *Development* **138**, 3043-3054.
Munjal, A., Philippe, J.-M., Munro, E. and Lecuit, T. (2015). A self-organized biomechanical network drives shape changes during tissue morphogenesis. *Nature* **524**, 351-355.
Rauzi, M., Lenne, P.-F. and Lecuit, T. (2010). Planar polarized actomyosin contractile flows control epithelial junction remodelling. *Nature* **468**, 1110-1114.
Sen, A., Nagy-Zsvér-Vadas, Z. and Krahn, M. P. (2012). Drosophila PATJ supports adherens junction stability by modulating Myosin light chain activity. *J. Cell Biol.* **199**, 685-698.
Sokolow, A., Toyama, Y., Kiehart, D. P. and Edwards, G. S. (2012). Cell ingression and apical shape oscillations during dorsal closure in Drosophila. *Biophys. J.* **102**, 969-979.
Solon, J., Kaya-Çopur, A., Colombelli, J. and Brunner, D. (2009). Pulsed forces timed by a ratchet-like mechanism drive directed tissue movement during dorsal closure. *Cell* **137**, 1331-1342.
Speck, O., Hughes, S. C., Noren, N. K., Kulikauskas, R. M. and Fehon, R. G. (2003). Moesin functions antagonistically to the Rho pathway to maintain epithelial integrity. *Nature* **421**, 83-87.
Tan, C., Stronach, B. and Perrimon, N. (2003). Roles of myosin phosphatase during Drosophila development. *Development* **130**, 671-681.
Toyama, Y., Peralta, X. G., Wells, A. R., Kiehart, D. P. and Edwards, G. S. (2008). Apoptotic force and tissue dynamics during Drosophila embryogenesis. *Science* **321**, 1683-1686.
Valencia-Expósito, A., Grosheva, I., Míguez, D. G., González-Reyes, A. and Martín-Bermudo, M. D. (2016). Myosin light-chain phosphatase regulates basal actomyosin oscillations during morphogenesis. *Nat. Commun.* **7**, 10746.
Vasquez, C. G., Tworoger, M. and Martin, A. C. (2014). Dynamic myosin phosphorylation regulates contractile pulses and tissue integrity during epithelial morphogenesis. *J. Cell Biol.* **206**, 435-450.
Vicente-Manzanares, M., Ma, X., Adelstein, R. S. and Horwitz, A. R. (2009). Non-muscle myosin II takes centre stage in cell adhesion and migration. *Nat. Rev. Mol. Cell Biol.* **10**, 778-790.
Xu, N., Bagumian, G., Galiano, M. and Myat, M. M. (2011). Rho GTPase controls Drosophila salivary gland lumen size through regulation of the actin cytoskeleton and Moesin. *Development* **138**, 5415-5427.
Yang, Y., Primrose, D. A., Leung, A. C., Fitzsimmons, R. B., McDermand, M. C., Missellbrook, A., Haskins, J., Smylie, A. L. S. and Hughes, S. C. (2012). The PP1 phosphatase flapwing regulates the activity of Merlin and Moesin in Drosophila. *Dev. Biol.* **361**, 412-426.
Zhang, L. and Ward, R. E. (2011). Distinct tissue distributions and subcellular localizations of differently phosphorylated forms of the myosin regulatory light chain in Drosophila. *Gene Expr. Patterns* **11**, 93-104.